RSC Advances

PAPER

View Article Online
View Journal | View Issue

Cite this: *RSC Adv.*, 2014, **4**, 13909

A facile method for fabrication of titanium-doped hybrid materials with high refractive index

Xibing Zhan,[a] Qingyu Xing,[a] Huijuan Liu,[a] Junying Zhang,*[ab] Jue Cheng*[ab] and Xin Lin[b]

Received 2nd November 2013
Accepted 27th February 2014

DOI: 10.1039/c3ra46359a

www.rsc.org/advances

This paper presents a facile route to prepare a series of high refractive index and homogeneous hybrid resins with titanium in the backbone by a non-hydrolytic sol–gel process. The confirmation of the condensation reaction and the formation of Si–O–Ti hetero-metal bonds in the hybrid resins were conducted by FT-IR spectroscopy, FT-Raman spectroscopy and liquid state ^{29}Si-NMR spectroscopy. In addition, the molecular weight and molecular size of the hybrid resin were characterized by MALDI-TOF MS and small-angle X-ray scattering (SAXS), respectively. These results show that the content of Si–O–Ti bridges, condensation degree of precursors and molecular weight and size of these hybrid resins increase depending on the TPT content from 0 to 30%. Moreover, the refractive index of the hybrid resin varied from 1.57 to 1.62 with increasing TPT content and the hybrid resin was thermally cured by hydrosilylation in the presence of a Pt catalyst to fabricate a transparent TSR hybrid film. These experimental results demonstrated that the physical and chemical properties of these hybrid films, such as visible transparency, surface roughness and surface energy, dielectric constant, thermal stability and glass transition temperature were investigated as a function of the chemical composition.

1. Introduction

Inorganic–organic hybrid materials (hybrimers) have been recognized as a new class of advanced materials and attracted considerable attention due to their versatile synthetic approaches and molecular tailing properties by controlling the inorganic and organic compositions.[1–3] Many attempts have been made in hybrid materials, especially high refractive index hybrimers because they have some potential applications in many advanced optoelectronic fabrications, such as substrates for display devices,[4] optical adhesives or encapsulants for light emitting diode (LED)[5] or organic light emitting diode (OLED),[6] antireflective coatings for advanced optical apparatus, *etc.*[7]

Oligosiloxane compounds, which are one of the most important members of hybrimer family and composed of a siloxane network by condensation and a cross-linked network formed by organic group polymerization at a molecular scale, are often transparent, more thermal and UV resistance than general polymers. Given these characteristics, they have been studied for potential optical materials or electronic packaging materials.[8–13] Vinyl-oligosiloxane-based hybrid materials have been fabricated in previous studies by hydrosilylation.[5] The hybrimers have excellent transparency and a relatively higher refractive index (around 1.56) compared to conventional methyl-type silicone materials (~1.4). However, in practical application, for instance, in high-brightness LED fabrication, the mismatch of the refractive index value between the semiconductor dies (GaN, $n = 2.5$) and organic encapsulants may result in low light extraction efficiency of the device. Therefore, it's essential to further increase the refractive index while maintaining molecular homogeneity so that they can be effectively utilized in LED devices and lamps.

Up to date, there are two fundamental methods to fabricate high refractive index oligosiloxane-based hybrid materials. The most popular one is introduction of high refractive index nanoparticles into matrix, such as TiO_2,[14–16] ZrO_2,[17] ZnS[18] *etc.* However, this approach may easily results in particle aggregation due to the largest specific surface energies of small nanoparticles and opacity because of the Rayleigh scattering of inorganic particles.[19] The other strategy is to incorporate inorganic domains into oligosiloxane matrix by chemical bond where inorganic elements are connected to organic moieties on a molecular lever.[20–27] But it's complicated and difficult to synthesize homogenous and stable oligosiloxane resin with Si–O–M (M = Ti, Zr, Al *etc.*) bonds by means of the conventional sol–gel process, because of the significant difference between the hydrolysis rates of the metal alkoxides and silicone analogues. Furthermore, there are large amounts of hydroxyl groups left in hybrid resins by using the hydrolytic sol–gel reaction, which may limit some applications for gate dielectric

[a]*Lab of Adhesives and In-situ Polymerization Technology, Key Laboratory of Carbon Fiber and Functional Polymers, Ministry of Education, Beijing University of Chemical Technology, Beijing 100029, China. E-mail: zjybuct@gmail.com; chengjue@mail.buct.edu.cn; Fax: +86 10 64425439; Tel: +86 10 64425439*

[b]*Changzhou institute of advanced material, Beijing University of Chemical Technology, Changzhou 213164, China*

of organic thin film transistors[28] or optical waveguides.[29] Thus, it becomes an important research area for fabrication of low hydroxyl values, stable and homogenous hetero-metal siloxane hybrid materials.

In the present study, in order to obtain homogenous and high refractive index hybrid resins, vinyltrimethoxysilane (VTMS), diphenylsilanediol (DPSD) and tetraisopropyl titanate (TPT) were employed to synthesize a series of oligosiloxane–titania hybrid resins by varying titanium contents *via* non-hydrolytic sol–gel process. And the synthesized oligosiloxane resin was thermally cured by hydrosilylation to fabricate titanium siloxane hybrid films. It was found that Si–O–Ti bonds were successfully introduced into the siloxane backbone and the refractive index of the hybrid resin increased according to the TPT content. In addition, the properties of hybrid films (such as transparency, dielectric constant, surface properties, TGA and glass transition temperature) also varied as a function of TPT content. In brief, given the comprehensive properties of hybrid resins, cured films and requirements for LED encapsulation materials, these synthesized materials have potential application for encapsulants for LED device, just like outer molded microlens of LED lamps.

2. Experimental

2.1 Materials

Vinyltrimethoxysilane (VTMS), tetraisopropyl titanate (TPT) and barium hydroxide hydrate ($Ba(OH)_2 \cdot H_2O$) (BH) were obtained from Sigma-Aldrich (USA). Diphenylsilanediol (DPSD) was purchased from TCI (Shanghai) Chemical Industry Development Co., Ltd. (China). The platinum catalyst (Pt content: 0.5%) was supplied by the AB Specialty silicones NanTong Co., Ltd. The branched cross-linking agent (hereafter shorted as TPHS) (0.31 wt% of the active hydrogen, refractive index: 1.51 at 25 °C) was obtained from Jiaxing United Chemical Co., Ltd, (China). The structure of cross-linker was shown below.

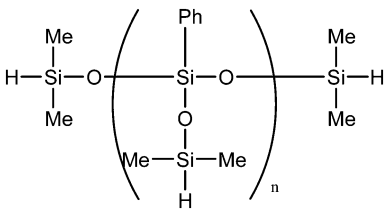

2.2 Characterization

^{1}H NMR and ^{29}Si-NMR analyses were carried out with a Bruker AV600 MHz nuclear magnetic resonance spectrometer (Bruker, Germany) at ambient temperature using $(CD_3)_2CO$ or $CDCl_3$ as solvent and tetramethylsilane (TMS) as an internal standard. FT-IR spectra were recorded on Alpha-T spectrometer (Bruker, Germany) with a resolution of 4 cm^{-1} at the range of 4000–400 cm^{-1} using KBr pellets and FT-Raman spectrometry (Renishaw inVia, UK) was used to examine the structure of TSR resin. Matrix-assisted laser desorption ionization time-of-flight (MALDI-TOF, AB 5800, USA) was used to study the distribution of the molecular weights of the TSR resins with 2,5-dihydroxybenzoic acid as a matrix. The molecular size of the synthesized TSR resins was measured by means of small-angle X-ray scattering (NanoSTAR, Germany). The scattering vector ranged from 0.01 and 0.2 Å and the sample was diluted by acetone in a mica window.

The refractive index of TSR resin was measured with an Abbe refractometer at 25 °C. The optical transmittance of the TSR hybrid film was tested on a Unico UV-4802 UV/vis spectrophotometer in a wavelength range of 300 to 800 nm. Dielectric spectroscopy was carried out by an impedance analyzer (Aglient 4294A) with frequency ranging from 10^2 to 10^6 Hz. An atomic force microscope (NanoScope IIIa, USA) was used to probe the surface morphology of the hybrid films and the area of about 10 μm^2 on the cured film was chosen for surface characterization. Root mean square roughness and average roughness (R_a) of the studied films were determined. The hydrophobicity of the hybrid film surface was evaluated by the contact angle measurement by using a contact angle meter (OCA-20, Dataphysics, Germany).

Thermal stability of each TSR hybrid sample (about 5 mg) was assessed on TG analyzer (NETZSCH TG209C, Germany) with heating rate of 10 °C min^{-1} from 25 to 900 °C under nitrogen atmosphere (N_2 flow rate: 20 mL min^{-1}). And the glass transition temperature was tested on differential scanning calorimeter (Perkin-Elmer DSC6000) with heating rate of 20 °C min^{-1} from −50 to 80 °C under nitrogen atmosphere.

2.3 Synthesis of titanium-doped oligosiloxane resin (TSR)

The precursors of VTMS and TPT were charged into a three-necked bottle and stirred with a magnetic stirrer for 5 min after tightly closing the mouth with rubber cork and then placed into 100 °C silicone oil-bath and then BH was added as a catalyst (0.2 mol% to the total silane and titanate compound) to promote the direct condensation reaction between the precursors. Subsequently, 40 wt% of *p*-xylene to the total precursors was added during the reaction and small amount (0.5 g) of DPSD was added with an interval of 5 minutes to prevent self-condensation and phase separation of DPSD. After complete addition of DPSD, the mixture was kept at 100 °C for another 6 h and then cooled it down to room temperature. The liquid was filtered to remove the catalyst by using 0.45 μm pore-sized Teflon filter. Also, by-products of the condensation reaction and residual solvent were removed on a rotary evaporator.

The molar ratio of precursor VTMS, DSPD and TPT was 4 : 6 : 0, 3 : 6 : 1, 2 : 6 : 2 and 1 : 6 : 3, corresponding to

Table 1 Composition of chemicals for synthesis of titanium-doped siloxane resin

Species	VTMS/ mmol	DSPD/ mmol	TPT/ mmol	$Ba(OH)_2 \cdot H_2O$/ mg	Vinyl content[30]/ (mol per 100 g)
TSR00	40	60	0	34.3	0.25
TSR10	30	60	10	34.3	0.186
TSR20	20	60	20	34.3	0.12
TSR30	10	60	30	34.3	0.058

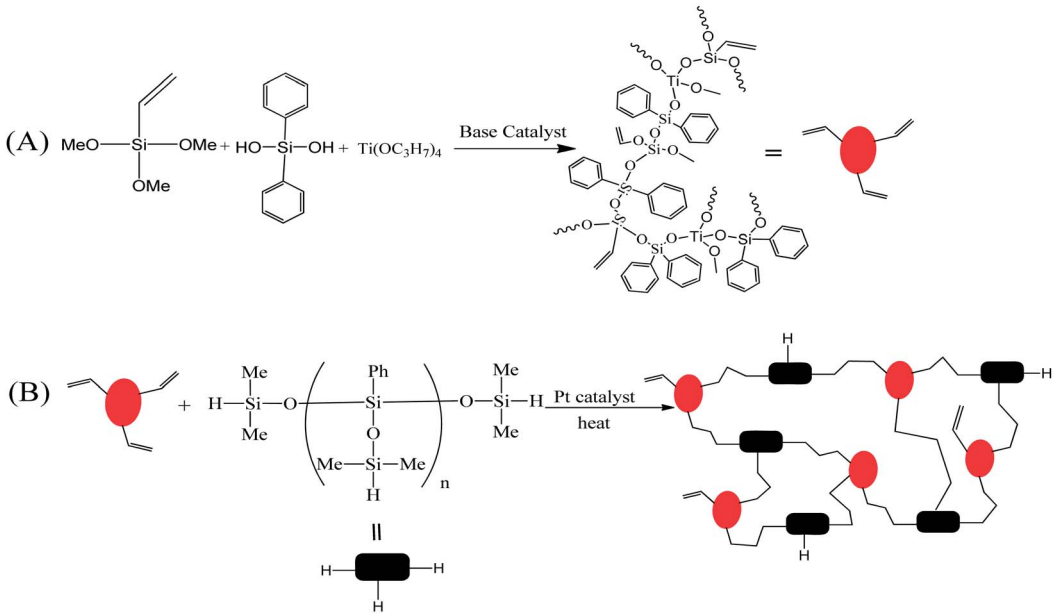

Scheme 1 Synthetic route of titanium-doped vinyl-oligosiloxane resin by non-hydrolytic sol–gel condensation reaction (A), and curing process of the titanium-doped oligosiloxane resin by hydrosilylation reaction (B).

condensation products denoted as TSR00, TSR10, TSR20, TSR30, respectively. The content of the DSPD precursor was fixed at 0.06 mol and TPT content was increased from 0 to 0.03 mol while the VTMS content was decreased from 0.04 to 0.01 mol, as listed in Table 1. The synthetic route was presented in Scheme 1(A).

2.4 Fabrication of the titanium-doped siloxane hybrid film

The TSR hybrid film was thermally cured by the hydrosilylation reaction between the vinyl group (Si–C═C) in TSR resin and the hydrogen bond (Si–H) in TPHS in the presence of Pt catalyst, result in a highly cross-linked network as demonstrated in Scheme 1(B). The TSR resin was mixed with TPHS in a 1 : 1 molar ration of Si–Vi to Si–H, and the Pt catalyst (about 10 ppm of total resin and cross-linker) was added. The mixture was degassed in vacuum and casted into a Teflon mold and followed by curing procedure at 150 °C for 2 h and 180 °C for 1 h in an oven.

3. Results and discussion

3.1 Characterization of titanium-doped hybrid resin (TSR)

Fig. 1 shows FT-IR spectra of TSR resins, presenting the evidence of the formation of Si–O–Ti bonds when TPT was introduced into the reaction mixture, and there is a notable difference among the TSR resins in spectra. It's detected that the peak in the region of 3200–3700 cm^{-1} was assigned to vibration of Si–OH, and the intensity of the bands at 2842 cm^{-1} which was assigned to the methoxy group (Si–OCH_3) gradually diminished with increment of TPT content. This means that the reaction between the precursors of VTMS and DSPD can be fully completed and TPT may be contribute to promote condensation reaction while Ti was also incorporated.[31] It has been reported that the metal alkoxide has catalytic effect in favor of the condensation and can prevent the formation of volatile species such as cyclic siloxanes.[32] Furthermore, a new absorption band located at 921 cm^{-1} which was assigned to the characteristic stretching vibration of Si–O–Ti hetero-metal bonds.[33] It

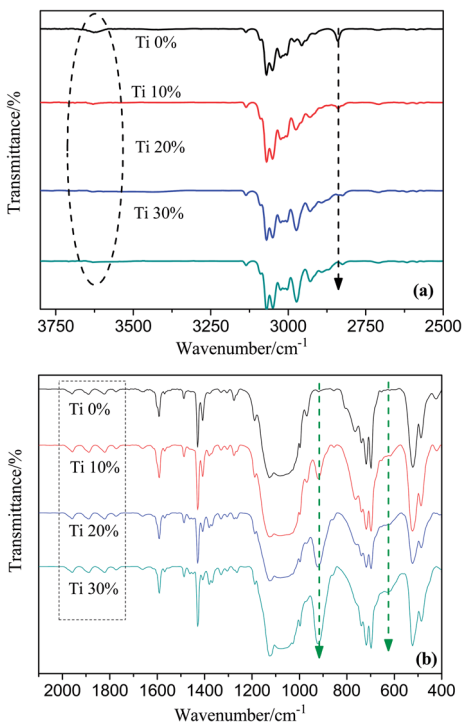

Fig. 1 FT-IR spectra of TSR resins according to the TPT content in a wavenumber range of 3750–2500 cm^{-1} (a), and 2100–400 cm^{-1} (b).

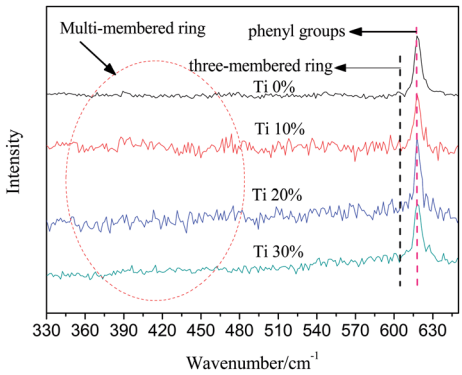

Fig. 2 FT-Raman spectra of TSR resins with different TPT content.

indicated successful incorporation of the titania segment into the siloxane backbone and the new band of 624 cm^{-1} may be attributed to Ti–O–C bonds of the precursor TPT, which suggested TPT didn't completely react with other precursors due to the steric effect of the bulky isopropoxy groups of TPT hindering the further reaction. As TPT content was increased from 0 to 30%, the intensity of Si–O–Ti bands relative to the intensity of Si–Ph bands (four consecutive peaks from 1774 to 1960 cm^{-1}) was gradually enhanced. This band intensity increment was consistent with the hypothesis that the formation of Si–O–Ti bonds was promoted depending on the amount of Ti. On the other hand, a sharp peak at 1128 cm^{-1} and a broad peak at around 1064 cm^{-1} are observed which represent the formation of Si–O–Si network by polycondensation. These two maxima are often observed in polysiloxane oligomers, polymers and networks.

The sol–gel condensation of different functional silanes can cause oligosiloxane to have linear, branched or multi-membered ring structure. Raman spectra of TSR resins of varying composition were employed to further confirm the structure of TSR resin and determine whether the polysiloxanes in the resin are linear or cycle. It's has already been reported that the three-membered ring peak of polysiloxane (*i.e.* hexaphenylcyclotrisiloxane) existed at 606 cm^{-1}, and multi-membered ring peaks of siloxanes were observed at a wavenumber of under 500 cm^{-1} in Raman spectra.[34,35] As shown in Fig. 2, the peaks at 606 and below 500 cm^{-1} almost can't be observed regardless of their compositions. This observation was explained by the fact that the cyclic siloxanes were prohibited in the presence of the basic catalyst or titanium alkoxides.[32,36] Based on the FT-Raman results, we can verify that there is no formation of cyclic siloxane rings or cage structures and the structures of TSR resins are linear or branched.

^{29}Si-NMR spectra of the synthesized oligosiloxanes are presented in Fig. 3. In the spectra, the band of the major condensed product is detected at D_2 and the intensity of the D_2 bands gradually increases with a reduction of the D_1 and T_2 bands as the TPT content is varied from 0 to 30%. Since the chemical shift of Si atoms which are directly bonded *via* oxygen with Ti shows a high field shift compared to corresponding Si–O–Si bonds, the peaks at −40.6 and −45 ppm are attributed to the Si atoms in the Si–O–*Si*–O–Ti bonds and Ti–O–*Si*–O–Ti bonds,

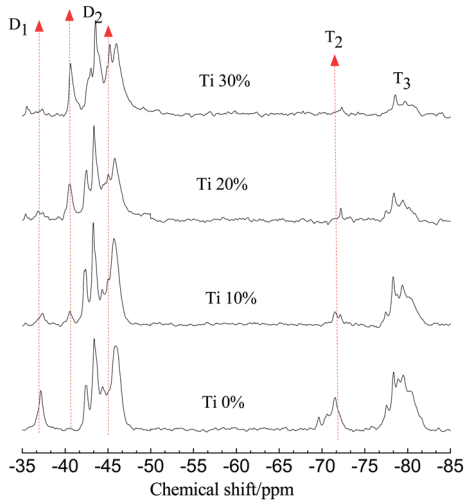

Fig. 3 ^{29}Si-NMR spectra of the TSR resins with diverse TPT content.

Table 2 Chemical shifts of silicon according to its bond states

Species	Chemical shifts (ppm)
D_0 (diphenyl dimethoxysilane)	~−29
D_0 (diphenylsilandiol)	~−34
D_1	−35 to −40
D_2	−40 to −48
T_1	−60 to −68
T_2	−70 to −75
T_3	−75 to −85

respectively.[37,38] Therefore, we could make a conclusion that Ti atom was successfully incorporated in the oligosiloxane structure. The degree of condensation (DOC) of TSR resin was calculated by the following eqn (1) based on the peak area of ^{29}Si-NMR spectra to show the condensation behavior depending on TPT content.[39] In NMR notation, D_n and T_n denotes Si atoms from DSPD and VSTM in the oligosiloxane structure, respectively, and the subscript '*n*' represent the number of Si–O bonds connected to Si atom (Table 2). The DOCs of TSR resins with different compositions are 91.24%, 95.14%, 95.26% and 95.77%, respectively. It implied that the TPT can contribute to not only promote the condensation between hydroxyl group of DPSD and methoxy group of VSTM, but also condensate between the isopropoxy group of TPT and the silanol group of DPSD.

$$\mathrm{DOC} = \frac{D_1 + 2D_2 + T_1 + 2T_2 + 3T_3}{2(D_0 + D_1 + D_2) + 3(T_0 + T_1 + T_2 + T_3)} \times 100 \quad (1)$$

As can be seen in Fig. 4, we analyzed the TSR molecular weight using MALDI-TOF spectra and observed that the molecular weight of TSR resins was mainly located at the range of 750–1250, 850–2200, 850–2400, 850–2700 corresponding to 0%, 10%, 20% and 30% TPT content, respectively. In order to increase the refractive index, it's important to increase the TPT content, thereby containing a large number of reactive groups

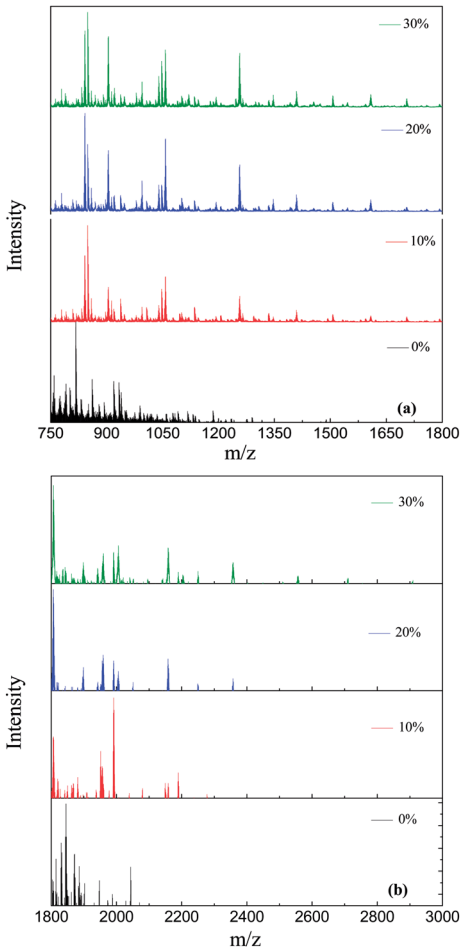

Fig. 4 MALDI-TOF spectra of the TSR resins with various TPT content.

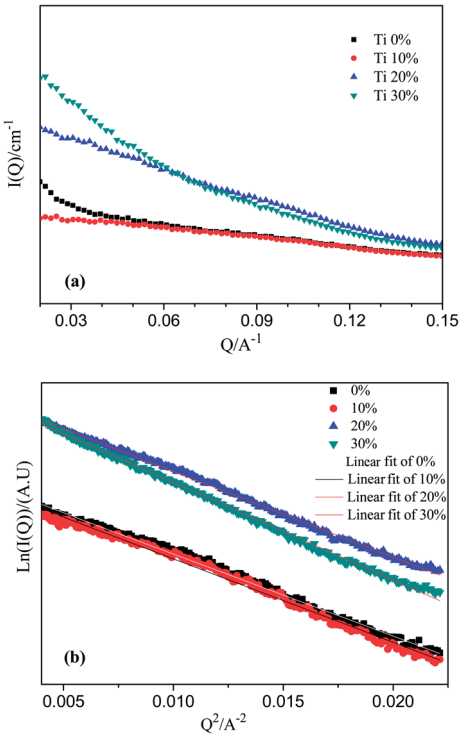

Fig. 5 Results of SAXS experiment of TSR resins of varying composition: (a) experimental SAXS data of the resins; (b) corresponding Guinier plots for the data.

which participate in the condensation reaction. The number of high molecular weight of TSR resins becomes more and more with the rise of TPT content from 0 to 30% and the MALDI-TOF MS peaks of TSR30 resins are shifted to peaks of species with high molecular weights compared to those of TSR00 resins. Therefore, we conclude that the TSR was successfully condensed to form a branched structure with high molecular weight, high Si–O–Ti content and low vinyl group content.

In this reaction, the solvent acts as a reaction medium to facilitate the formation of Si–O–Ti bonds which is due to the reaction of Si–OH and Ti–OR. Because Ti is more electrophilic than Si, Si–OH reacts more slowly with Si–OR. Also, Ti–O–Ti bonds may be formed owning to hydrolysis of Ti–OR by traces of moisture or by ligand exchange with Si–OH. Ti–O–Ti bonds can also derive from exchange reaction between Si–O–Ti bonds to give rise to Si–O–Si and Ti–O–Ti.[40] However, we can't observe the peaks at 1630 and 630 cm^{-1} which are typical asymmetrical and symmetrical stretching vibration absorption peaks of the Ti–O–Ti bond in the FT-IR spectra.[41,42] In virtue of electronegative activities between Si and Ti, the formed Si–O–Ti bonds are much more polarizable compared to Si–O–Si bonds. More polarized bonds induce preferred nucleophilic attack of silanol group of DPSD.[43] The formation of the hetero-metal bonds is consistently promoted and self-condensation is relatively prohibited once Si–O–Ti bonds commences.[37] As a result, Si–O–Ti can be dispersed homogenously in the oligosiloxane structure.

3.2 Molecular size and distribution of titanium-doped vinyl-oligosiloxane resins

SAXS is a very useful technique to characterize the molecular sizes of polymers on the order of 10 Å or larger. It turns out, however, even when the shape is unknown or when the shape is irregular and not describable in simple terms, that the scattering function still follows a certain universal form, in the limit of small Q, which is given by the Guinier Law[44]

$$I(Q) = \rho_0^2 \gamma^2 \exp\left(-\frac{1}{3}Q^2 R_g^2\right) \quad (2)$$

$I(Q)$ is the scattering intensity, Q is the scattering vector, ρ_0 is the scattering length density of the resin, γ is the molar volume of the resin, and R_g is the gyration radius of the resin.

The experimental SAXS data recorded for TSR resins with different TPT content are plotted as the scattered intensity $I(Q)$ *versus* the scattering vector Q in Fig. 5(a), and the size of TSR resins were calculated with the radius of gyration (R_g) which was determined by the following eqn (3) from the Guinier plots in the Guinier region of the SAXS spectra (Fig. 5(b)) and the gradients of the Guinier plots negatively increase with TPT content, indicating that the molecular size of the resin becomes larger. And the real molecular size of the resins can be

Table 3 Radius of gyration (R_g), Diameter of sphere shape ($2R_s$), and length of rod-like shape (R_r) calculated from SAXS data

Sample	R_g (nm)	$2R_s$ (nm)	R_r (nm)
TSR00	1.56	4.03	5.4
TSR10	1.58	4.08	5.47
TSR20	1.60	4.13	5.54
TSR30	1.71	4.42	5.92

estimated from R_g from the Guinier plots by following eqn (4) and (5), depending on their shapes.[44]

$$\ln[I(Q)] = A - \frac{1}{3}Q^2 {R_g}^2 \quad (3)$$

$$\text{Sphere shape } R_g = \sqrt{\frac{3}{5}} R_s \quad (4)$$

$$\text{Thin rod-like shape } R_g = \sqrt{\frac{1}{12}} R_r \quad (5)$$

R_s is the radius of the spherical shape and R_r is the length of the thin rod-like shape. The calculated $2R_s$, R_r and R_g are listed in Table 3. Real molecular size of the oligosiloxane depending on their shapes is estimated from R_g. Since the size of the spherical shape ($2R_s$) is the smallest and the size of the thin rod-like shape (R_r) is the largest, the molecular size in the TSR resins is in the range from 4 nm ($2R_s$) to 6 nm (R_r). It's indicated the TSR resin was a nanocomposite which consists of the nano-sized oligomers with diameters of 4–6 nm. In addition, it's confirmed that the molecular size become much larger with increasing TPT content. We measured MALDI-TOF MS to support the SAXS results and confirm that TSR resins have species with high molecular weight and size in rise of TPT content.

3.3 Optical, and electrical properties of TSR resin and TSR hybrid film

A high refractive index (n) is an important factor for encapsulation materials of LED devices. Compared to conventional LED encapsulants (n < 1.5), the refractive index of TSR resins markedly increase up to 1.622 in the presence of Ti. As shown in Fig. 6, it can be observed that the refractive index varies from 1.578 to 1.622 with an increase in TPT content. The refractive index can be predicted through Lorentz–Lorenz eqn (6),[45] which expresses the correlation among the refractive index (n), the molecular refraction (R), molecular weight (M), and molecular volume (V) of the polymer repeating unit. In eqn (6), R/M can be further termed as molar refraction (R_M), which is the sum of atomic and group refraction of the components composing the polymer repeating unit. Similarly, M/V can be defined as the reciprocal of molar volume (V_M).

$$\frac{n^2-1}{n^2+2} = \frac{R}{M}\rho = \frac{R}{M}\frac{M}{V} = \frac{R_M}{V_M} \quad (6)$$

Thus, eqn (6) is transformed into eqn (7)

$$n = \sqrt{\frac{1+2(R_M/V_M)}{1-(R_M/V_M)}} \quad (7)$$

According to eqn (7), the refractive index of the materials is directly proportional to the electronic polarizability and density. That's to say, it can be effectively enhanced by increasing the molecular or group polarizability or decreasing the molecular molar volume. In general, the refractive index of polymer can be adjusted by introducing some functional groups with larger molar refraction (R_M), such as phenyl (R_M = 25.5), halogen (R_M = 6–9) except for fluorine, sulfur (R_M = ~8), *etc.*[46] In addition, metal element or metallic oxides, such as nano-TiO_2 (anatase (n = 2.45); rutile (n = 2.7)), nano-ZrO_2 (n = 2.1) are also beneficial for increasing the refractive indices of polymers. In this paper, the control of RI has been achieved by the synergic effects of phenyl groups and Ti element which are both combined into the polymer backbone. The phenyl groups in DSPD show high electronic polarizability.[47] Furthermore, a sufficient amount of highly polarizable Si–O–Ti bonds and a more condensed inorganic network are formed when Ti contend reaches 30%, as already verified by the FT-IR and ^{29}Si-NMR analysis. It can be clearly seen that in the studied TPT content range, the refractive index of TSR resin is proportional to the molar concentration of TPT and there was a good linear fitting relationship between the polymer refractive index and TPT content. These results indicate that the refractive index of these hybrimers can be easily tuned by changing the TPT content for various applications.

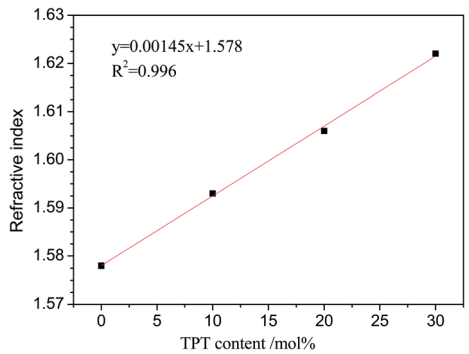

Fig. 6 Dependence of refractive index of TSR resins on the TPT content.

On the other hand, optical transparency is also vital to LED devices and lamps. The optical transmission spectra for the hybrid film with different TPT molar fractions were shown in Fig. 7 and the color of films gradually turned from colorless to yellow in the rise of TPT from 0 to 20%. In addition, it was observed that the film exhibit good transparency in the region of 500–800 nm regardless of the TPT content. However, the transmittance of the TSR cured films sharply decrease in the region of 350–500 nm as the TPT content increases, even the transmittance reach down to 0% with higher TPT content. This phenomenon may be explained by the fact that the color of

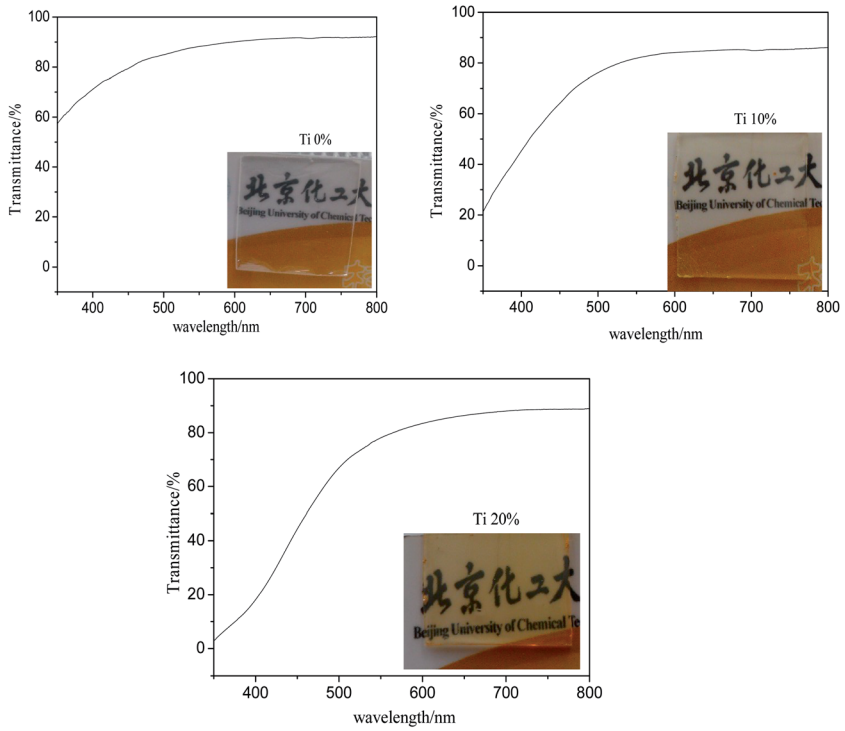

Fig. 7 Optical transmission spectra of TSR hybrid film (2 mm thickness) with different TPT content at the wavelength of 400 to 800 nm.

the films affects the transmittance. As we all know, when the visible light come in through yellow and transparent substance, blue light (400–500 nm) will be absorbed so that the transmittance in the blue light region was very much lower as the color of cured film was become yellower and yellower. Here, we can use yellow index (YI) to reflect the degree of yellowness, which was defined as follow equation.

$$\mathrm{YI} = \frac{T_{680\ \mathrm{nm}} - T_{420\ \mathrm{nm}}}{T_{560\ \mathrm{nm}}} \times 100\%$$

which $T_{420\ \mathrm{nm}}$, $T_{560\ \mathrm{nm}}$, $T_{680\ \mathrm{nm}}$ represents the transmittance at the wavelength of 420 nm, 560 nm and 680 nm, respectively. The yellow index of TSR00, TSR10 and TSR20 was 0.188, 0.38 and 0.75, respectively. The results showed that the yellow index became much greater, the color was turned more yellow. Therefore, the film with lower TPT content is more transparent and the color is much lighter than that higher TPT content.

Meanwhile, it's well known that surface properties such as surface energy and roughness are of the most importance in some applications (such as outer molded optical microlens for LED lamps or gate insulator in OTFTs[48]). From Fig. 8(A), it's observed that the water contact angle of the TSR hybrid film was about 101.4°, 98.9° and 96.5° corresponding to 0%, 10% and 20%TPT content, respectively, which indicates that it has a hydrophobic surface. The hydrophobic surface of the hybrimer film is attributed to the vinyl and phenyl groups grafted to the oligosiloxanes networks and the water contact angle decreased with increase of TPT content due to reduce of VTMS content in the TSR resins. In addition, the surface roughness of the TSR thin film containing different TPT was investigated by AFM (Fig. 8(B)). The surface roughness is very smooth as low as around 4 Å of root mean square (rms) roughness, which is similar to that of the SiO_2 grown thermally on single crystal silicon.[49] This means that TSR film has good surface performance and the TPT content makes little impact on the surface properties.

As we all know, dielectric constant of polymer is closely related with displacement polarization, orientation polarization and interface polarization in the applied electric field.[50] Fig. 9 represents the variation of the dielectric constant of TSR resins as a function of the frequency at ambient temperature, and the dielectric constant of each resin is almost independent on the frequency, indicating that TSR resins have good stability of dielectric constant on frequency. However, it's found that the dielectric constant of TSR hybrid film depends on the TPT content and changes from 3.2 to 3.9 at 1 MHz. These data can be interpreted by the difference in the chemical structure of TSR resins and cross-linking density of the cured film. On the one hand, similar to the case of the refractive index, more polar Si–O–Ti bonds as compared to Si–O–Si bonds can increase the dielectric constant according to the amount of TPT. Moreover, TSR00 hybrid film has high cross-linking density owing to TSR00 resin has many cross-linking points, while other two hybrid films (TSR10 and TSR20) have low cross-linking degrees and have some residual polarizable groups (such as isopropoxy groups), indicating that the orientation polarization of dipoles are easy to take place in cured TSR10 and TSR20 rather than TSR00 network, so TSR00 hybrid film has the lowest dielectric constant among the three resin. Therefore, we can also incorporate various precursors and tune the dielectric constant for

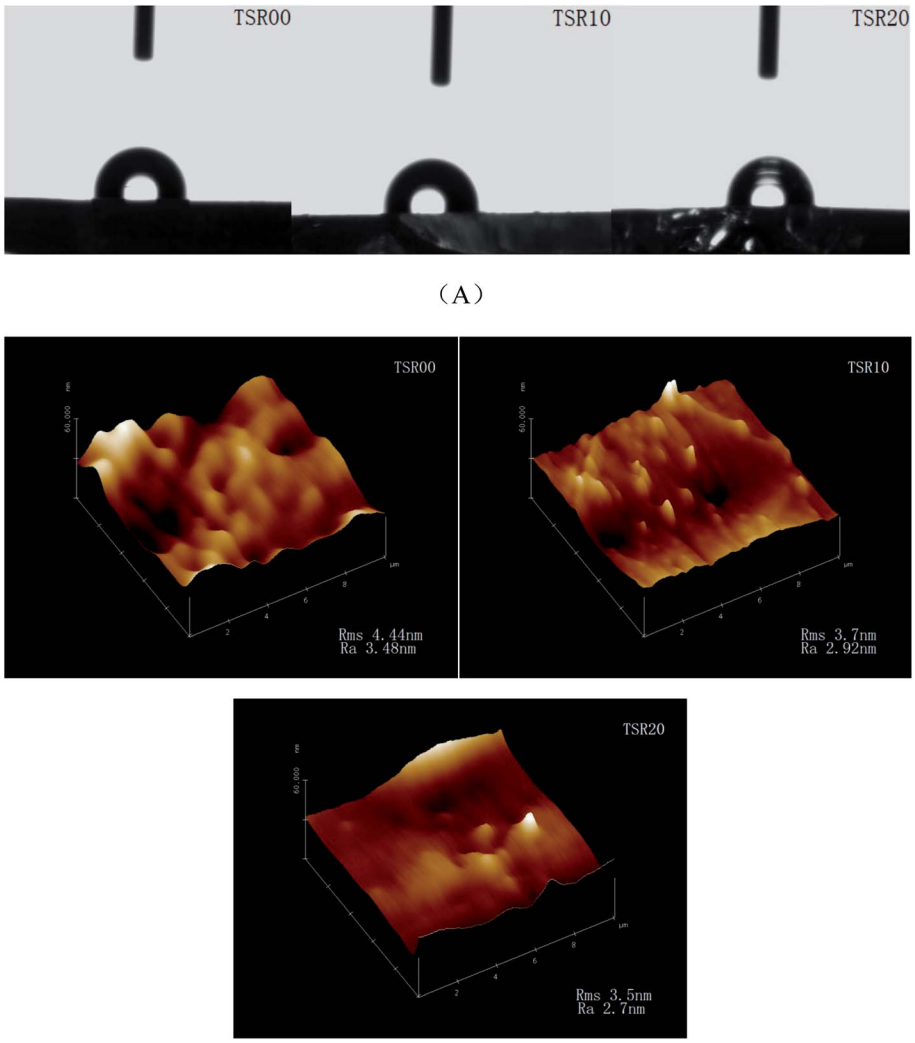

Fig. 8 (A) Contact angle measurement for TSR film; (B) AFM surface image of TSR film with different content TPT.

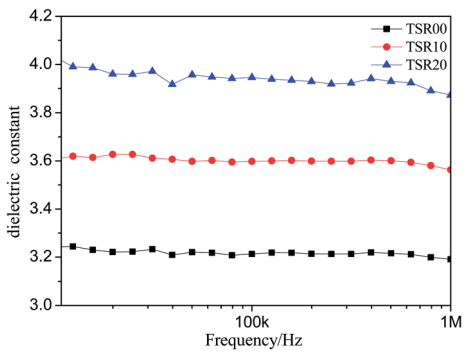

Fig. 9 Dependence of dielectric constant on frequency of TSR00, TSR10 and TSR20 film.

different application for optoelectronic devices such as sulfur inside oligosiloxane to increase the dielectric constant ($\zeta = 4.15$)[51] or fluorine inside oligosiloxane to reduce the dielectric constant ($\zeta = 2.54$).[52]

3.4 Thermal gravimetric analysis (TGA)

To assess the thermal stability of TSR hybrid films, TGA was carried out under the nitrogen atmosphere to avoid the effect of moisture in air on the stability of the Si–O–Ti bonds.[53] Fig. 10

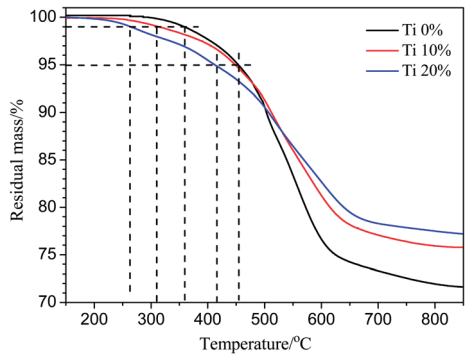

Fig. 10 TGA profile of TSR hybrid film with various TPT content at a heating rate of 10 °C min^{-1} (measured under N_2 atmosphere).

Table 4 TG and glass transition temperature (T_g) results of TSR hybrimers with different composition

Sample	$T_{1\%}$[a] (°C)	$T_{5\%}$[b] (°C)	$T_{10\%}$[c] (°C)	R_w[d] (%)	T_g[e] (°C)
TSR00	355	453	503	71.7	42.5
TSR10	305	448	512	75.6	45.2
TSR20	260	415	507	77.3	53.8

[a] Temperature at 1% weight loss. [b] Temperature at 5% weight loss. [c] Temperature at 10% weight loss. [d] Residual char at 850 °C. [e] Glass transition temperature (T_g).

demonstrated the TGA profiles of each TSR hybrimer containing various TPT content, and mass loss temperature of different compositions can be summarized and compared in Table 4. The whole weight loss can be roughly separated by two temperature regions, namely, between 200 and 500 °C, and from 500 to 700 °C. In the first stage (200 to 500 °C), the weight loss is believed to be a result of the volatilization of the organic components which are the by-products from thermal polycondensation reaction as well as the carbonization or the combustion of the organic groups, that is to say, this weight reduction is due to the loss of carbon, hydrogen, and oxygen, and the second stage was the characteristic decomposition between 500 and 700 °C, in which the steep weight loss is probably regarded as the break and rearrangement of Si–O–Si and Si–O–Ti on the main chain and the further combustion of the remnant organic groups. As we all know, the thermal stability of thermosetting polymer almost lied on the structure of main chain and crosslinking density. The decomposition temperature corresponding to different TSR cured hybrids decreased at the first stage as the content of TPT increased. This phenomenon can be attributed to the fact that there are some residual unreacted groups such as isopropoxyl groups connected to the Ti atoms that can be thermally decomposed or further condensed under increasing temperature circumstance and the reduce of amount of chemical cross-linking points. However, the decomposition temperature increased with the rise of TPT content when the temperature was above 550 °C because there are much more Si–O–Ti units (160 kJ mol^{-1}) which are of higher bond dissociation energy in comparison with Si–O–Si units (108 kJ mol^{-1}) in the main chain.[54,55]

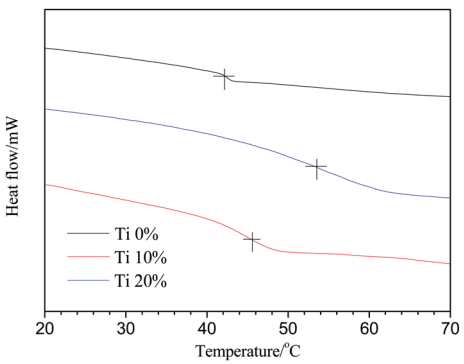

Fig. 11 DSC curves of TSR hybrimer film with different TPT content at a heating rate of 20 °C min^{-1} under nitrogen flow.

Additionally, the char yields also increased with increment of TPT content at the temperature of 850 °C. According to the TGA data, TSR20 cured film has the maximum char yield more than 77%, which is about 5% higher than the TSR00 cured hybrids as a comparison. The achievement of such high char yields may be due to the highly thermally stable Si–O–Si units and Si–O–Ti units in the thermosets, which can be formed as amorphous silica and titanium dioxide in the pyrolytic degradation.

On the other hand, glass transition temperature (T_g) is an important parameter that gives the information about the structure of cross-linked polymers. And it's well known that glass transition is generally ascribed to the segmental motion of the polymeric networks, and T_g is determined by the degree of freedom for the segmental motion, cross-linking and entanglement constraints, and the packing density of the segments.[56] The DSC traces of TSR cured samples are demonstrated in Fig. 11 and obtained results are summarized in Table 4. All hybrid films exhibit an increased T_g from 42.5 to 53.8 °C compared with pure silicone resin, which indicates that the mobility of the polymer chains in the hybrid compounds is constrained. This is because TPT is a tetra-functional precursor which will help to form a low degree of cross-linked three-dimensional network reacting with other alkoxysilane precursors. In addition, the cure of hybrid resin will further form a dense cross-linking network, which is conducive to prevent the segmental motion. These resulted in a high packing density for the polymeric network, and thus, a relatively high T_g was gained.

4. Conclusion

This research demonstrates the synthesis of TSR resins and the fabrication of TSR films by hydrosilylation. Using a modified sol–gel process that requires no water, the nano-sized and transparent oligosiloxane resins with Si–O–Ti units in the backbone were successfully prepared in a single-step condensation reaction. Moreover, the refractive index of TSR resins increase from 1.57 to 1.62 and the molecular size of TSR resin ranges from 4–6 nm according to the TPT content. The hybrid films exhibit good transparency in the visible region, smooth surface, good hydrophobicity and have higher dielectric constant (~3.9 at 1 MHz) compared to convention oligosiloxane resins which are attributed to the higher polarizability of Si–O–Ti bonds. In addition, the second decomposition temperature and glass transition temperature (T_g) increase with an increasing of TPT content mainly because of introduction of some Ti–O bonds and the augment of cross-linking density. In short, we can control the physical–chemical properties of hybrid resin and films by means of adjusting TPT or VSTM content and these hybrimers are promising candidates for encapsulants for LED device, just like outer molded microlens of LED lamps.

Acknowledgements

The authors express their gratitude to National High Technology Research and Development Program of China (no. 2011AA03A109) and Applied Basic Research Plan of Changzhou,

China (no. CJ20120011). In additional, we'd like to give our special thanks to the reviewers and editor for reading the manuscript and giving some constructive recommendations.

Notes and references

1 R. M. Laine, *J. Mater. Chem.*, 2005, **15**, 3725.
2 C. Sanchez, B. Julian, P. Belleville and M. Popall, *J. Mater. Chem.*, 2005, **15**, 3559.
3 H. Althues, J. Henle and S. Kaskel, *Chem. Soc. Rev.*, 2007, **36**, 1454.
4 T. Nakamura, H. Fujii, N. Juni and N. Tsutsumi, *Opt. Rev.*, 2006, **13**, 104.
5 J. S. Kim, S. C. Yang and B. S. Bae, *Chem. Mater.*, 2010, **22**, 3549–3555.
6 D. W. Mosley, K. Auld, D. Conner, J. Gregory, X. Q. Liu, A. Pedicini, D. Thorsen, M. Wills, G. Khanarian and E. S. Simon, *Proc. SPIE*, 2008, **6910**, 691017.
7 K. C. Krogman, T. Druffel and M. K. Sunkara, *Nanotechnology*, 2005, **16**, S338.
8 R. Buestrich, F. Kahlenberg and M. Popall, *J. Sol-Gel Sci. Technol.*, 2001, **20**, 181.
9 J. Y. Bae, Y. H. Kim, H. Y. Kim, Y. W. Lim and B. S. Bea, *RSC Adv.*, 2013, **3**, 8871.
10 S. C. Yang, S. Y. Kwak, J. H. Jin, J. S. Hu and B. S. Bea, *J. Mater. Chem.*, 2012, **22**, 8874.
11 S. C. Yang, J. S. Kim, J. H. Jin, S. Y. Kwak and B. S. Bae, *J. Appl. Polym. Sci.*, 2011, **122**, 2478.
12 K. H. Jung, J. Y. Bae, S. J. Park and B. S. Bae, *J. Mater. Chem.*, 2011, **21**, 1977.
13 S. C. Yang, S. Y. Kwak, J. H. Jin and B. S. Bae, *ACS Appl. Mater. Interfaces*, 2009, **1**, 1585.
14 P. Tao, Y. Li, A. Rungta, A. Viswanath, J. N. Gao and L. S. Schadler, *J. Mater. Chem.*, 2011, **21**, 18623.
15 D. H. Nguyen, H. N. Kim and D. S. Lee, *J. Nanosci. Nanotechnol.*, 2012, **12**, 4207.
16 K. W. Lem, D. H. Nguyen, H. N. Kim and D. S. Lee, *J. Nanosci. Nanotechnol.*, 2011, **11**, 7202.
17 S. K. Lee, H. J. Shin, S. M. Yoon, D. K. Yi, J. Y. Choi and U. Paik, *J. Mater. Chem.*, 2008, **18**, 1751.
18 N. Sergienko, D. Godovsky, B. Zavin, M. J. Lee and M. J. Ko, *Nanoscale. Res. Lett.*, 2012, **7**, 181.
19 H. I. Elim, B. Cai, Y. Kurata, O. Sugihara, T. Kaino, T. Adschiri and N. Kambe, *J. Phys. Chem. B*, 2009, **113**, 10143.
20 D. P. Dworak and M. D. Soucek, *Macromol. Chem. Phys.*, 2006, **207**, 1220.
21 H. P. Xiang, J. F. Ge, S. H. Cheng, H. M. Han and S. W. Cui, *J. Sol-Gel Sci. Technol.*, 2011, **59**, 635.
22 L. Tellez, *J. Mater. Sci.*, 2003, **38**, 1773.
23 N. Yamada, I. Yoshinaga and S. Ktayama, *J. Mater. Chem.*, 1997, **7**, 1491.
24 W. C. Chen, L. H. Lee, B. F. Chen and C. T. Yen, *J. Mater. Chem.*, 2002, **12**, 3644.
25 W. C. Chen, W. C. Liu, P. T. Wu and P. F. Chen, *Mater. Chem. Phys.*, 2004, **83**, 71.
26 N. Yamada, I. Yoshinaga and S. Katayama, *J. Sol-Gel Sci. Technol.*, 2000, **17**, 123.
27 S. Ivanovici, C. Rill, T. Koch, M. Puchberger and G. Kickelbick, *New J. Chem.*, 2008, **32**, 1243.
28 Z. Bao, V. K uck, J. A. Rogers and M. A. Paczkowski, *Adv. Funct. Mater.*, 2002, **12**, 526.
29 M. Oubaba, M. Smaihi, P. Eteinne, P. Coudray and Y. Moreau, *J. Non-Cryst. Solids*, 2003, **318**, 305.
30 Z. Y. Li, *Industry Analysis of Silicone Compounds*, Chemical Industry Press, Beijing, 1979, p. 74.
31 X. S. Luo, C. J. Zha and B. L. Davies, *J. Sol-Gel Sci. Technol.*, 2004, **32**, 297.
32 S. Dire, F. Babonneau, G. Carturan and J. Livage, *J. Mater. Chem.*, 1992, **2**, 239.
33 C. C. Chang and W. C. Chen, *J. Polym. Sci., Part A: Polym. Chem.*, 2001, **39**, 3419.
34 A. Pasquarello and R. Car, *Phys. Rev. Lett.*, 1998, **80**, 5145.
35 T. Nakano, N. Mura and A. Tsuzumitani, *Jpn. J. Appl. Phys*, 1995, **34**, 1064.
36 Y. J. Eo, T. H. Lee, S. Y. Kim, J. K. Kang and B. S. Bea, *J. Polym. Sci., Part B: Polym. Phys.*, 2005, **43**, 827.
37 D. Hoebbel, T. Reinert and H. Schmidt, *J. Sol-Gel Sci. Technol.*, 1996, **7**, 217.
38 D. Hoebbel, T. Reinert and H. Schmidt, *J. Sol-Gel Sci. Technol.*, 1996, **6**, 139.
39 Y. J. Eo, J. H. Kim, J. H. Ko and B. S. Bea, *J. Mater. Res.*, 2005, **20**, 401.
40 L. Crouzet, D. Leclercq, P. H. Mutin and A. Vioux, *Chem. Mater.*, 2003, **15**, 1530.
41 W. C. Du, H. T. Wang and W. Zhong, *J. Sol-Gel Sci. Technol.*, 2005, **34**, 227.
42 J. Yu, Z. Feng and L. Xu, *Chem. Mater.*, 2001, **13**, 994.
43 F. D. Monte, P. Cheben, C. P. Grover and J. D. Mackenzie, *J. Sol-Gel Sci. Technol.*, 1999, **15**, 73.
44 R. J. Roe, *Methods of X-ray and Neutron Scattering in Polymer Science*, Oxford University Press, New York, 2000, p. 155.
45 J. C. Seferis, in *Polymer Handbook*, ed. J. Brandrup and E. H. Immergut, Wiley, New York, 3rd edn, 1989.
46 J. G. Speight, *Lange's Handbook of Chemistry*, McGraw-Hill, 16th edn, 2005.
47 E. S. Kang, J. U. Park and B. S. Bae, *J. Mater. Res.*, 2003, **18**, 1889.
48 C. G. Choi and B. S. Bae, *Org. Electron.*, 2007, **8**, 743.
49 C. G. Choi and B. S. Bae, *J. Nanosci. Nanotechnol.*, 2008, **8**, 4679.
50 J. Fan, X. Hu and C. Y. Yue, *J. Polym. Sci., Part B: Polym. Phys.*, 2003, **41**, 1123.
51 J. S. Kim, S. C. Yang, H. J. Park and B. S. Bae, *Chem. Commun.*, 2011, **47**, 6051.
52 J. H. Oh, S. Y. Kwak, S. C. Yang and B. S. Bae, *ACS Appl. Mater. Interfaces*, 2010, **2**, 913.
53 D. Hoebbel, M. Nacken, H. Schmidt, V. Huch and M. Veith, *J. Mater. Chem.*, 1998, **8**, 171.
54 S. Gong, C. Hu, W. Wang and Q. Liu, *Acta Polym. Sin.*, 2006, **25**, 180.
55 X. M. Wang, Y. H. Wu, Z. F. Hao, J. Yu and L. Yu, *Chem. Res. Chin. Univ.*, 2010, **26**, 851.
56 H. Wang, Y. Zhang, L. Zhu, Z. Du, B. Zhang and Y. Zhang, *Thermochim. Acta*, 2012, **529**, 29.

